"Effective" Negative Surface Tension: A Property of Coated Nanoaerosols Relevant to the Atmosphere

Purnendu Chakraborty and Michael R. Zachariah*

Department of Mechanical Engineering and Department of Chemistry and Biochemistry, University of Maryland, College Park, Maryland

Atmospheric aerosols play a very important role in atmospheric processes and have a major influence on the global climate. In this paper, we report results of a molecular dynamics study on the unique properties of organic-coated water droplets. In particular, we find that, for particles preferring an inverted micelle structure, the lower chain–chain interaction, with increasing radial distance from the water–organic interface, results in a negative internal radial pressure profile for the organic layer. As a result, a coated particle behaves as though the surface tension is "negative" and implies that such a particle will inherently have an inverse Kelvin vapor pressure effect, resulting in increased water condensation.

Introduction

Aerosol particles are ubiquitous in the earth's atmosphere and have a major influence on global climate and perhaps climate change. They can locally either intensify or moderate the effects of the greenhouse gases through scattering or absorption of both incoming solar radiation and thermal radiation emitted from the earth's surface. Aerosols also act as cloud condensation nuclei (CCN) and thereby affect the radiative properties of clouds.[1] Water-soluble surfactants are known to affect droplet activation by lowering the surface tension and thus changing the critical drop radius and can conceptually be described by Kohler theory.[2] However, it has recently been discussed that insoluble surfactants may be important components of Marine aerosols. It has been shown[3,4] using time-of-flight secondary mass spectrometry (TOF–SIMS) that fatty acids reside on surfaces of sea-salt aerosols. In a subsequent work,[5] the ubiquity of fatty acid population on a variety of continental aerosols was reported.

A conceptual model has been suggested[6,7] for the composition, structure, and atmospheric processing of organic aerosols. The organic materials that coat the aerosol particles are surfactants of biological origin. It is believed that the organic aerosol prefers an "inverted micelle" structure consisting of an aqueous core that is encapsulated in an inert, hydrophobic organic monolayer. The surfactants lie with their polar heads inserted into the ionic aqueous core and with their hydrophobic hydrocarbon tails exposed to the atmosphere. Indeed, for surfactants with packing parameter ($v/a_0 l_c$, where v is hydrocarbon chain volume, l_c is the critical chain length, and a_0 is the optimal surface area occupied by each head group) greater than 1, the inverted micelle structure is favored.[8] For such inverted micelle structures, with negative curvature modulus, the surface energy has an extra term $1/2 k_b R^2$, where k_b is the curvature modulus and R is the radius of the particle, making the surface energy negative.[9] Recently, Wyslouzil et al.[10] has shown, using small angle neutron scattering, evidence for surface segregation of organic/water systems, and Wilemski[11] using Monte Carlo methods mapped out the stability regions of binary water/organic droplets.

Understanding the structure and properties of these coated aerosols is important, as they may significantly affect the processing of water vapor in the atmosphere, cloud formation, and the radiation balance to the earth.

It is well-known that the presence of surfactants on a planar water surface reduces the surface tension.[9,12] In this paper, we carry out molecular dynamics calculations of the pressure profile and the corresponding surface tension of the coated particles. The results indicate that the organic coating on a curved surface of such a droplet is under negative pressure. Using a simple model, we illustrate that this negative pressure is a manifestation of the curved surface. As a result, the particle seems to behave in a manner consistent with a "negative surface tension". We explain the physical significance of this result in the context of water vapor processing.

Computational Model

The structures of these particles are computed using a "coarse graining" potential approach to simplify the representation of water and the organic coating. The coarse-grained methods have their shortcomings, but their utility for surfactant systems has been demonstrated.[13] For surfactant systems, it has been suggested that coarse-grained models can be made sufficiently accurate to mimic specific surfactants. For the inverted micelle model, we follow the coarse-grained model developed by Shelley et al.[13–15] This model mimics the key physical or structural features known from experiments of atomistic simulations. The nonbonded interactions were modeled using the Lennard-Jones $m-n$ potential, which has the form

$$V(r) = k\epsilon \left[\left(\frac{\sigma}{r} \right)^m - \left(\frac{\sigma}{r} \right)^n \right] \tag{1}$$

Here, r is the distance between two different sites, ϵ is the potential well depth, and σ is the distance at which this potential is zero.

For water, a spherically symmetric site has been chosen, referred to as a "W"-site, to represent a "loose grouping of three water molecules". Interactions between W sites are described using a Lennard-Jones 6–4 potential. This potential function
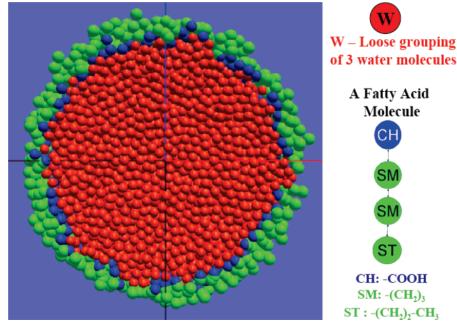
---

* Corresponding author. mrz@umd.edu.

Figure 1. Cross-sectional view of the coated particle and a single fatty acid molecule.

TABLE 1: Nonbonded Interactions

site	type	σ (Å)	ϵ/k_B (K)
W−W[a]	LJ 6−4	4.58	212.10
W−CH[b]	LJ 6−4	4.58	212.10
CH−CH[c]	LJ 12−6	4.22	110.7
W−SM[a]	LJ 9−6	4.49	130.57
CH−SM[b]	LJ 9−6	4.49	130.57
W−ST[a]	LJ 9−6	4.49	200.00
CH−ST[b]	LJ 9−6	4.49	200.00
SM−SM[a]	LJ 9−6	4.40	123.00
SM−ST[a]	LJ 9−6	4.40	188.40
ST−ST[a]	LJ 9−6	4.40	288.06

[a] Values obtained from ref 13. [b] Assume W−CH = W−W; CH−SM = W−SM; CH−ST = W−ST. [c] Value obtained from ref 22.

TABLE 2: Harmonic Bonded Interactions

bond	r_0 (Å)	k_r/k_B (K)
SM−SM[a]	3.67	6600
SM−ST[a]	4.53	6600
CH−SM[b]	3.67	6600

[a] Values obtained from ref 13. [b] Assume CH−SM = SM−SM.

TABLE 3: Angle Cosine Interactions

angle	θ_0 (rad)	k_θ/k_B (K)
CH−SM−SM[a]	π	1150
SM−SM−ST[b]	π	1150

[a] Assume CH−SM−SM = SM−SM−ST. [b] Values obtained from ref 13.

has a relatively wide potential minimum, permitting liquid−vapor existence for a wide range of temperatures. ϵ_{WW} is chosen such that the melting temperature of a slab of W sites arranged on an fcc lattice is 212.1 K. σ_{WW} is chosen so as to produce the density of 1 g/cc at 303.15 K.

A fatty acid molecule is shown in Figure 1. Harmonic bond length potentials of the form

$$V(r) = \frac{k_r}{2}(r - r_0)^2 \qquad (2)$$

are used to link together the adjacent beads in a fatty acid molecule.

Bond angle potentials are needed to maintain proper chain stiffness and overall length, and for this, we use a cosine angle potential

$$V(\theta) = k_\theta[1 - \cos(\pi - \theta)] \qquad (3)$$

Nonbonded interactions between two beads from different fatty acid molecules were modeled by the Lennard-Jones 9−6 potential. The potential parameters are listed in Tables 1−3.

Simulation Procedure

The simulations were run on either a Linux cluster or on an IBM SP3 running up to eight processors. The trajectories of all the atoms were determined by integrating the equations of motion[16] using the velocity form of Verlet algorithm with rescaling at each time step to achieve temperature control. A time step of 2 fs was typically used to ensure energy conservation, and the Verlet neighbor list with parallel architecture[17] was employed in all the simulations. All simulations were done in a spherical cavity with "spherical boundary conditions".[18] The radius of the cavity was taken to be 27.5 nm (for particles of sizes 5−7 nm) so as not to influence the particle properties.

The first step in the equilibration procedure was to prepare an equilibrated pure water particle consisting of 8192 W sites at 254 K. An initial simple cubic configuration was taken, and velocity was generated corresponding to a temperature of 100 K. The temperature was then slowly raised until the structure melted. The radial distribution function at 254 K confirmed a liquid state. At a higher temperature (about 275 K), the droplet started evaporating. Unless otherwise noted, all simulations took place at the constant temperature of 254 K.

The next step was to coat the spherical water droplet with fatty acid molecules. A fatty acid molecule was placed on each surface W site (CH site attaching to the surface W, and the rest of the surfactant molecule radially outward). The coated particle was then equilibrated at 254 K. For the last step in the preparation process, the simulation was switched to a constant energy calculation. If the average temperature of the particle deviated by more than 10 K, the equilibration process was
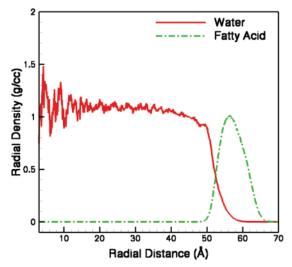
"Effective" Negative Surface Tension

J. Phys. Chem. A, Vol. 111, No. 25, 2007 **5461**

Figure 2. Radial density profile of the coated particle.

Figure 3. Radial pressure profiles of the bare and coated particles. Also included is the density profile of fatty acid in a coated particle.

repeated until the particle temperature deviated by less than 10 K. The fatty acid molecules did not leave the surface of the equilibrated particle at the simulation temperature, and the droplet was stable throughout the process of equilibration and later when we computed the normal pressure. Figure 1 shows a cross-sectional view of the equilibrated coated particle. It has a core−shell structure as has been predicted for model aqueous organic droplets using density functional theory,[11] and consistent with the experimental work of Wyslouzil et al.[10]

Density, Pressure, and Surface Tension Calculations

Density and Pressure. Both density and pressure profiles were computed as a function of r, the distance from the center of mass.

To compute density, we introduced subspherical shells at a distance of $\delta r = 0.02\sigma_W$ from each other where σ_W is the potential parameter for W−W interaction. For density calculations, we considered a spherical shell of thickness δr at a distance r from the center of mass. Then, the density at distance r is given by the mass of all the sites in that shell divided by the volume of the shell. The density profile of the coated particle is as in Figure 2.

On the grounds of symmetry, the pressure tensor can be written as[18,19]

$$\mathbf{p}(r) = p_N(r)[\mathbf{e_r e_r}] + p_T(r)[\mathbf{e_\theta e_\theta} + \mathbf{e_\varphi e_\varphi}] \quad (4)$$

where $\mathbf{e_r}$, $\mathbf{e_\theta}$, and $\mathbf{e_\varphi}$ are orthogonal unit vectors, and r is the distance from the center. The normal component of the Irving−Kirkwood pressure, $p_N(r)$, is given by $p_N(r) = p_K(r) + p_U(r)$, where $p_K(r)$ and $p_U(r)$ are the kinetic and configurational terms, respectively, and are given by

$$p_K(r) = k_B T \rho(r)$$

$$p_U(r) = S^{-1} \sum_k f_k \quad (5)$$

where k_B is the Boltzmann constant, T is the particle temperature, S is the area of the spherical surface of radius r, and f_k is the normal component of the force between two sites acting across the surface S. The radial pressure profiles of the bare and coated particles are as in Figure 3. We used the same spherical shells as above to compute $p_N(r)$. The radial density and normal pressure were averaged over 500 snapshots collected over
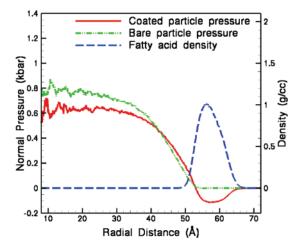
100 ps. The important point is that, for the coated particle, the coating was found to be under negative pressure, i.e., tension (compare the pressure profiles in Figure 3 with the fatty acid density). The implication of this to surface properties is discussed later.

Surface Tension. We computed the surface and interfacial tension following Widom et al.[19] We consider a drop of phase α immersed in phase β, which in turn is immersed in phase γ. The system is described by polar coordinates r, θ, and ϕ. The system under discussion is bounded by two concentric spheres, of radii R^α (which lies in phase α) and R^γ (in phase γ) (and the sphere of radius R^β lies in phase β). Two arbitrary surfaces of radii R_1 and R_2 separate the three phases.

Following the arguments in ref 19, for the phase α to be in equilibrium with phase β, we get

$$\gamma_i = \int_{R^\alpha}^{R^\beta} \left(\frac{r}{R_1}\right)^2 dr[p_N(r) - p_T(r)]$$

The general condition of mechanical equilibrium leads to $p_T(r) = p_N(r) + (r/2)(dp_N(r)/dr)$. So, we get

$$\gamma_i = \int_{R^\alpha}^{R^\beta} \left(\frac{r}{R_1}\right)^2 dr\left[-\frac{r}{2}\frac{d}{dr} p_N(r)\right] \quad (6)$$

The Laplace−Young equation gives $\gamma_i = \frac{1}{2}R_1(p_\alpha - p_\beta)$, which leads to

$$\gamma_i^3 = -\frac{1}{8}(p_\alpha - p_\beta)^2 \int_{R^\alpha}^{R^\beta} r^3 \frac{dp_N(r)}{dr} dr \quad (7)$$

where p_α is the bulk pressure in phase α, and so forth. Similarly, for phases β and γ to be in mechanical equilibrium with each other, we arrive at a relation similar to eq 7 with appropriate integration limits.

Equation 7 gives the mechanical route for the calculation of surface tension. As has been pointed out,[18] neither the thermodynamical approach nor the mechanical approach is without limitations. However, it has been shown by Thompson et al.[18] that the values of the surface tension computed via both these routes have the same trends and differ by less that 10%. So, the current value of the surface tension can be taken as a good approximation to the thermodynamic surface tension.

Discussion

Pressure. The radial pressure profile of the coated particle, presented in Figure 3, shows that the interior of the particle is
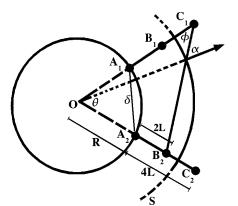
Figure 4. A simple model to illustrate the existence of negative pressure.

Figure 5. Plot of the normal pressure vs the radius of the droplet keeping the length of the chains fixed.

under compression, as expected from the Laplace−Young equation. However, the pressure profiles for the bare and the coated particles are noticeably different in that the coated particle has a significant negative pressure for the coating.

We can probe the physical manifestation of this with a simple model. We consider a sphere of radius R (a droplet of water). We assume that the fatty acid molecules have one polar head (A_i) and two hydrocarbon beads $(B_i$ and $C_i)$. The length of each such molecule is $4L$ (Figure 4). These molecules are considered to be rigid with the polar head binding to the water surface and the hydrocarbon beads radially outward. We further assume that these molecules are distributed evenly on the water surface so that the distance between any two A_i's is always δ. The only force acting between sites is that between the beads B_i and C_j with $i \neq j$, and the force is between the nearest neighbors only. Let F_N be the normal component of the force across the surface S, which is of radius $R + 3L$. Then, $F_N = F_d \cos \alpha$, where F_d is the magnitude of the force acting between B_i and C_j. We want to compute the pressure across the surface S.

Next, consider three adjacent fatty acid molecules on the surface of the sphere. We have an equilateral triangle with the vertices on the surface of the sphere. The area of this triangle is $A_T = (\sqrt{3}/4)\delta^2$. Total surface area of the sphere is $4\pi R^2$. So, the number of such triangles is

$$N_T = \frac{4\pi R^2}{A_T} = \frac{16\pi R^2}{\sqrt{3}\delta^2}$$

(δ being small compared to R, we can ignore the contribution from the spherical excess).

The number of A_i's on the surface of the sphere $\approx N_T$, and the number of nearest neighbors of each fatty acid molecule is 6, such that the normal component of the pressure across S is

$$p_N(r = R + 3L) = \frac{6F_N \times N_T}{4\pi(R + 3L)^2} \tag{8}$$

Taking $\delta = (\sigma_0/\sqrt{2})$ (so that, for large R, the force between B_i and C_j is zero) and keeping L fixed at $(\delta/2)$, we vary R from $10 \times \delta$ to $1000 \times \delta$ with an increment of $10 \times \delta$. From Figure 5, we see that the normal pressure is in fact negative initially and approaches zero for large R (i.e., a flat surface). In other words, the effect is less pronounced for large particles and/or for smaller chains.

This result indicates that the radial pressure profile for a core−shell-like particle, where the coating molecules are tethered to
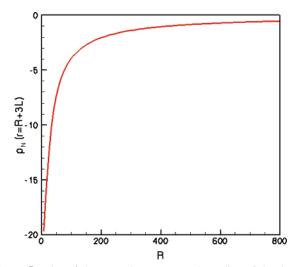
the core will result in, by simple geometric considerations, a decrease in density with increasing distance from the core. This decreasing density should always result in a coating under tension.

Surface Tension. From the MD computed pressure profiles we obtain (using eq 7 with $p_\alpha = 0.77$ kbar, $p_\beta = 0$ kbar, and integrating from $r = 16$ Å to $r = 60$ Å), a surface tension of 166 mJ/m² for the bare particle.

For the coated particle, with $p_\beta = p_2 = -0.116\,67$ kbar, $p_\gamma = p_3 = 0$ kbar, and integrating from $r = 57$ Å to $r = 70$ Å, we get the surface tension $\gamma_s = -36.36$ mJ/m². i.e., "negative surface tension". The interfacial surface tension ($p_\alpha = p_1 = 0.652$ kbar, $p_\beta = p_2 = -0.116\,67$ kbar, and integrating from $r = 20$ Å to $r = 57$ Å) is $\gamma_i = 176.233$ mJ/m².

There are two interfaces in our system, one between water and fatty acid and the second between fatty acid and vacuum. A negative surface tension would imply that the particle would tend to increase its interface either by deformation (so that it is no longer spherical) or by mixing. Since the fatty acid is essentially insoluble (see the density plot of the coated particle and Figure 1), the only way to increase the area of the surface would be by deformation. However, the water−fatty acid interfacial tension is positive, implying that this interface always tries to reduce its energy by reducing its surface area by maintaining a spherical shape (see the cross-sectional view of the coated particle in Figure 1). So, there is a competition between the two tensions in which the water−fatty acid interfacial tension is of higher magnitude. Hence, the particle stays spherical and forces the coating to maintain a spherical shape. Thus, we have a stable spherical particle with an "effective" negative surface tension.

We also computed the normal pressure profile for the coated particle in the presence of water vapor. For this, 56 W sites were introduced in the spherical cavity, outside the coated particle, and the system was allowed to evolve for 500 ps. At the end of the equilibration period, the density and pressure were evaluated. Some of the W sites were absorbed into the particle, with the rest remaining outside in the vapor phase. None of the W sites were seen to stick to the surface, and so the pressure profile was not affected by water vapor absorption (the coating remains under tension). The computed pressure profile is identical (within statistical noise) to the pressure profile obtained earlier (Figure 3).
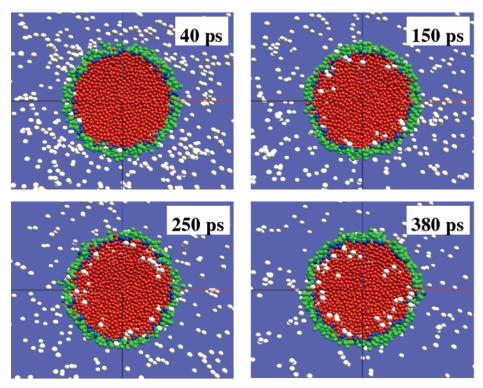
"Effective" Negative Surface Tension

J. Phys. Chem. A, Vol. 111, No. 25, 2007 **5463**

Figure 6. Snapshots of the coated particle processing water.

Next, we turn to the potential implications of this result to the atmosphere where these structures are most likely to be found. To study the effect of the coating on condensation, 1352 vapor "W" sites were introduced into the spherical cavity, outside the particle, with random velocity (corresponding to the temperature of 254 K). As observed in Figure 6, vapor-phase water sites are absorbed into the particle, indicating the propensity of the particle to process water even though it has a hydrophobic surface. We believe that this condensation observed is due to the effective negative surface tension of the particle.

The equilibrium vapor pressure over a small particle is higher than that over a flat surface and is given by the Kelvin equation[20]

$$\ln \frac{p}{p_S} = \frac{2\gamma\bar{v}}{r_p RT} \tag{9}$$

where p is the actual pressure of the vapor, p_S is the equilibrium vapor pressure for planar surface, r_p is the droplet radius, γ is the surface tension, $\bar{v}$ is the molar volume of the liquid, R is the gas constant, and T is the temperature. Here, we use the Kelvin equation for qualitative explanation, since there is no other formalism that is suitable for a graded structure of the type being considered here. There is of course a body of understanding for the vapor pressure of a drop containing a nonvolatile solute.[2,21] Li et al.[2] studied the effect of soluble surfactants on the activation of aerosol particles. They developed a model that partitions the surfactant between the droplet's gas−liquid interface and bulk volume, and computed Kohler curves with surfactant partitioning affecting the surface tension but not the Raoult effect. Sorjamaa et al.[21] extended this study to include effects of surfactant partitioning affecting both the surface tension and the Raoult effect. However, in both these works, the surface tension was assumed to follow the Szyskowski equation of state for large particles, the radius being on the order of 100 nm. In our case, we have computed the surface tension of a much smaller particle (radius ∼6−7 nm), but the far more

important and fundamental difference is that, in contrast to the studies discussed above, the surfactant in our case is insoluble and is on the surface of the droplet to form an inverted micelle, rather than being dispersed within the droplet (as is evident from the density profile of the coated particle). As a result, the water vapor sees only a hydrophobic surface and not the presence of water inside. For the water vapor, the particle might very well be a pure droplet. And so, an expression containing positive and negative terms resulting in the Kohler curves is not really appropriate. It is in that context that the Kelvin equation for a pure droplet comes in. Normally, for a small particle, $p > p_S$. However, if γ were in fact negative, we would have $p < p_S$, i.e., *the vapor pressure of the particle is reduced due to the organic coating, and thus a coated particle would act as an enhanced condensation surface.* This obviously poses many interesting questions as to how an oil surface can process water and its importance in the atmosphere.

When a sufficiently large amount of water vapor has assimilated into the water nucleus of the particle, the inverted micelle surface structure would be degraded. The surface would now consist of both water and fatty acid. For such partially coated particles, the surface tension needs to be recomputed and the Raoult term added to the Kelvin equation. In a future work, we plan to study the effect of surface coverage on the surface tension of the particle.

The implication of this result is that organic-coated water may be a very efficient substrate to process water vapor and as such act as a surprisingly efficient water/cloud condensation nucleus. This result suggests that an experimental effort be undertaken to assess the nature of this effect and the propensity of these structures to process water and other molecules.

Conclusion

Molecular dynamics simulations using a coarse-grained model were carried out to study the properties of fatty acid

coated water droplets. The particle exhibits a core−shell structure. It was found that the organic coating is under tension and as a result behaves as if it has a negative surface tension. As a result, the particle can process water even though it has a hydrophobic surface and hence acts as an enhanced condensation surface.

References and Notes

(1) Buseck, P. R.; Posfai, M. Airborne minerals and related aerosol particles: Effects on climate and the environment. *Proc. Natl. Acad. Sci. U.S.A.* **1999**, *96*, 3372.

(2) Li, Z.; Williams, A. L.; Rood, M. J. Influence of soluble surfactants properties on the activation of aerosol particles containing inorganic solute. *J. Atmos. Sci.* **1998**, *55*, 1859.

(3) Tervahattu, H.; Hartonen, K.; Kerminen, V.-M.; Kupiainen, K.; Aarnio, P.; Koskentalo, T.; Tuck, A. F.; Vaida, V. New evidence of an organic layer on marine aerosols. *J. Geophys. Res. (Atmos.)* **2002**, *107*, D7.

(4) Tervahattu, H.; Juhanoja, J.; Kupiainen, K. Identification of an organic coating on marine aerosol particles by TOF-SIMS. *J. Geophys. Res. (Atmos.)* **2002**, *107*, D16.

(5) Tervahattu, H.; Juhanoja, J.; Vaida, V.; Tuck, A. F.; Niemi, J. V.; Kupianien, K.; Kulmala, M.; Vehkamaki, H. Fatty Acids on Continental Sulfate Aerosol Particles. *J. Geophys. Res.* **2005**, *110*, D06207.

(6) Ellison, G. B.; Tuck, A. F.; Vaida, V. Atmospheric Processing of Organic Aerosols. *J. Geophys. Res.* **1999**, *104*, D9, 11633.

(7) Dobson, C. M.; Ellison, G. B.; Tuck, A. F.; Vaida, V. Atmospheric aerosols as prebiotic chemical reactors. *Proc. Natl. Acad. Sci. U.S.A.* **2000**, *97*, 11864.

(8) Israelachvili, J. *Intermolecular & Surface Forces*, 2nd ed.; Academic Press: London, 1991.

(9) Safran, S. *Statistical Thermodynamics of Surfaces, Interfaces and Membranes*; Addison-Wesley: Reading, MA, 1994.

(10) Wyslouzil, B. E.; Wilemski, G.; Strey, R.; Heath, C. H.; Dieregsweiler, U. Experimental evidence for internal structure in aqueous-organic nanodroplets. *Phys. Chem. Chem. Phys.* **2006**, *8*, 54−57.

(11) Li, J. S; Wilemski, G. A structural phase diagram for model aqueous organic nanodroplets. *Phys. Chem. Chem. Phys.* **2006**, *8*, 1266.

(12) Facchini, M. C.; Decesari, S.; Mircea, M.; Fuzzi, S.; Loglio, G. Surface Tension of Atmospheric Wet Aerosol and cloud/fog droplets in relation to their organic carbon content and chemical composition. *Atmos. Environ.* **2000**, *34*, 4853−4857.

(13) Shelley, J. C.; Shelley, M. Y.; Reeder, R. C.; Bandyopadhyay, S.; Klein, M. L. A coarse grained model for phospholipid simulations. *J. Phys. Chem. B* **2001**, *105*, 4464−4470.

(14) Shelley, J. C.; Shelley, M. Y.; Reeder, R. C.; Bandyopadhyay, S.; Moore, P. B.; Klein, M. L. Simulations of phospholipids using a coarse grain model. *J. Phys. Chem. B* **2001**, *105*, 9785−9792.

(15) Lopez, C. F.; Moore, P. B.; Shelley, J. C.; Shelley, M. Y.; Klein, M. L. Computer simulation studies of biomembranes using a coarse grain model. *Comput. Phys. Commun.* **2002**, *147*, 1−6.

(16) Allen, M. P.; Tildesley, D. J. *Computer Simulation of Liquids*; Oxford: U.K., 2004.

(17) Plimpton, S. Fast Parallel Algorithms for Short-Range Molecular Dynamics. *J. Comput. Phys.* **1995**, *117*, 1−19.

(18) Thompson, S. M.; Gubbins, K. E.; Walton, J. P. R. B.; Chantry, R. A. R.; Rowlinson J. S. A Molecular Dynamics study of liquid drops. *J. Chem. Phys.* **1984**, *81*, 530.

(19) Rowlinson, J. S.; Widom, B. *Molecular Theory of Capillarity*; Clarendon: Oxford, U.K., 1982.

(20) Friedlander, S. K. *Smoke, Dust and Haze: Fundamentals of Aerosol Dynamics*; Oxford University Press: Oxford, U.K., 2000.

(21) Sorjamaa, R.; Svenningsson, B.; Raatikainen, T.; Henning, S.; Bilde, M.; Laakonsen, A. The role of surfactants in Kohler theory reconsidered. *Atmos. Chem. Phys.* **2004**, *4*, 2107−2117.

(22) Moller, M. A.; Tildesley, D. J.; Kim, K. S.; Quirke, N. Molecular Dynamics Simulations of a Langmuir-Blodgett Film. *J. Chem. Phys.* **1991**, *94*, 8390.